

ANALYSIS OF PAPR REDUCTION IN OFDM SYSTEMS

A Thesis

by

HAOSI LIU

Submitted to the Office of Graduate and Professional Studies of
Texas A&M University
in partial fulfillment of the requirements for the degree of

MASTER OF SCIENCE

| | |
|---------------------|-------------------|
| Chair of Committee, | Scott L. Miller |
| Committee Members, | Alex Sprintson |
| | Krishna Narayanan |
| | Aakash Tyagi |
| Head of Department, | Miroslav Begovic |

December 2019

Major Subject: Electrical Engineering

Copyright 2019 Haosi Liu

ABSTRACT

This thesis considers the long-standing problem of Peak-to-Average-Power Ratio (PAPR) reduction in OFDM systems. Due to the nonlinear amplifiers commonly used, OFDM signals often will be distorted when they are transmitted. Many methods have been proposed before to reduce the PAPR: block coding, clipping, and insertion are the most common. They all change the signal by adjusting the signal or its input data. In this thesis, 3 methods that take a different approach are discussed: Gradient Descent, Newton's Method, and Single Peak Suppression. These methods aim to move the constellation points in order to lower the peak power. Different OFDM system parameters regarding the number of subcarriers and the constellation size are considered and the results show that all three methods can reduce the PAPR. Single Peak Suppression is the fastest and the simplest method overall. Gradient Descent can produce well suppressed signal at a medium complexity. While Newton's Method can reach low PAPR in the fewest iterations, its computational complexity for each iteration makes it the least efficient overall to carry out.

DEDICATION

To my dad, my mom, and my little brother

ACKNOWLEDGEMENTS

I would like to express my sincerest gratitude to my advisor, Dr. Scott L. Miller, for his constant support and guidance in me throughout this research. His ideas and patience helped me grow so much as a researcher and have inspired me to do so much more than I previously thought I could.

I am also grateful for Dr. Alex Sprintson, Dr. Krishna Narayanan, and Dr. Aakash Tyagi, who took time out of their busy schedule to serve on my committee.

Thanks to all my friends, colleagues, faculty and staff for making the last six years at Texas A&M University special.

Lastly, I would like to thank my parents and my brother for supporting me throughout my academic career, and for their love and encouragement.

CONTRIBUTORS AND FUNDING SOURCES

Contributors

This work was supervised by a thesis committee consisting of Professor Scott Miller [advisor], and Professors Alex Sprintson and Krishna Narayanan of the Department of Electrical and Computer Engineering and Professor Aakash Tyagi of the Department of Computer Science and Engineering.

All work for the thesis was completed independently by the student.

Funding Sources

This work was done independently without outside financial support.

TABLE OF CONTENTS

| | Page |
|--|------|
| ABSTRACT | ii |
| DEDICATION | iii |
| ACKNOWLEDGEMENTS | iv |
| CONTRIBUTORS AND FUNDING SOURCES..... | v |
| TABLE OF CONTENTS | vi |
| LIST OF FIGURES..... | viii |
| LIST OF TABLES | ix |
| CHAPTER I INTRODUCTION | 1 |
| CHAPTER II OFDM ANALYSIS..... | 3 |
| OFDM Overview..... | 3 |
| Initial Analysis | 5 |
| CHAPTER III METHODS | 6 |
| Previous Suppression Methods | 6 |
| Basic Suppression Technique..... | 7 |
| Single Peak Suppression | 8 |
| Description | 8 |
| Calculation and MATLAB Implementation..... | 9 |
| Gradient Descent Method..... | 10 |
| Description | 10 |
| Problem Modification and Calculation | 10 |
| MATLAB Implementation..... | 14 |
| Newton's Method..... | 15 |
| Description | 15 |
| Calculation and MATLAB Implementation..... | 16 |
| CHAPTER IV RESULTS | 17 |
| SPS Overshot..... | 17 |

| | |
|----------------------------|----|
| PAPR Reduction | 18 |
| Reduction Efficiency | 21 |
| Method Complexity..... | 22 |
| Error Rate | 24 |
| Additional Results..... | 26 |
| CHAPTER V CONCLUSION | 31 |
| REFERENCES..... | 32 |

LIST OF FIGURES

| | Page |
|--|------|
| Figure 1 OFDM System Model..... | 3 |
| Figure 2 Part of a randomly generated signal before and after reduction. The threshold was the average final PAPR of Gradient Descent and Newton’s Method. All respective PAPRs are also shown. (72 subcarriers with QPSK) | 19 |
| Figure 3 CCDF of the PAPR of the 10,000 signals shown in Table 4..... | 21 |
| Figure 4 PAPR after each iteration of Gradient Descent and Newton’s Method..... | 22 |
| Figure 5 Error rate of the constellation points before and after reduction (72 subcarriers with QPSK). EVMs: -19.44dB (GD), -18.68dB (NM), -18.12dB (SPS). | 25 |
| Figure 6 Part of a randomly generated signal before and after reduction (72 subcarriers with 16QAM). The respective PAPR is also shown. | 26 |
| Figure 7 Error rate of the constellation points before and after reduction (72 subcarriers with 16QAM). EVMs: -18.57dB (GD), -18.69dB (NM), -17.50dB (SPS) | 27 |
| Figure 8 Part of a randomly generated signal before and after reduction (180 subcarriers with 16QAM). The respective PAPR is also shown. | 28 |
| Figure 9 Error rate of the constellation points before and after reduction (180 subcarriers with 16QAM). EVMs: -22.56dB (GD), -23.20dB (NM), -21.11dB (SPS). | 28 |
| Figure 10 Error rate of the constellation points before and after Gradient Descent (300 and 1200 subcarriers with 16QAM). EVMs: -24.78dB (300), -30.80dB (1200)..... | 29 |
| Figure 11 Part of a randomly generated signal before and after reduction (72 subcarriers with 16QAM, $\epsilon = 0.2$). The respective PAPR is also shown..... | 30 |
| Figure 12 Error rate of the constellation points before and after reduction (72 subcarriers with 16QAM, and $\epsilon = 0.2$). EVMs: -28.58dB (GD), -28.67dB (NM), -26.13dB (SPS). | 30 |

LIST OF TABLES

| | Page |
|--|------|
| Table 1 PAPR Statistics for QPSK, 16QAM, 64QAM, 256QAM with 72 subcarriers..... | 5 |
| Table 2 Iteration statistics for different values of p . 10,000 randomly generated signals were reduced with each value of p , and all with the threshold of 4dB..... | 17 |
| Table 3 Final PAPR statistics for different values of p . 10,000 randomly generated signals were reduced with each value of p , and all with the threshold of 4dB..... | 18 |
| Table 4 PAPR statistics post reduction by all three methods. 10,000 randomly generated signals were used. SPS used the average of the averages of Gradient Descent and Newton's Method as the threshold and 0.5dB as the overshoot amount..... | 20 |
| Table 5 Approximated number of operations for each category (real addition/subtraction; real multiplication/division; exponential/logarithmic and square roots) for all methods (including clipping and filtering). N = number of subcarriers, F = Finite Impulse Response (FIR) Filter Length | 23 |
| Table 6 Average time for each method's total time recorded in MATLAB. | 24 |

CHAPTER I

INTRODUCTION

As the use of wireless electronics becomes more of a necessity in everyday lives, it is as expected that the technology associated with them grows and adapts to new standards. A key component to such technology is the signals that are transmitted. There are many aspects to a signal that would determine and affect how it will be received and interpreted at the receiver. One of the most important aspects is interference. Whether it is with other signals, or by some environmental factor, interference will distort the transmitted signal and could potentially change the core message that was intended by the original signal.

Orthogonal Frequency Division Multiplexing (OFDM) is a commonly used modulation method that could reduce problems caused by long delay spreads [1], its high spectral efficiency also makes the method ideal for higher data transmission rates [2]. OFDM has made its way into many telecommunication standards and practices. In the 1990s, systems such as radio LANs (local area networks) [3], DAB (digital audio broadcasting) [4], and DTTB (digital television terrestrial broadcasting) [5] all began using OFDM. Since the 2000, with the rise of cellphone network and wireless internet, more modern telecommunication practices such as 4G/LTE, and numerous WLAN (wireless local area networks) Wi-Fi protocols have started to make use of OFDM. Many aspects of OFDM have been studied: signal to noise ratio (SNR) vs Spectral

efficiency [6], throughput [7], etc. By itself or comparing with other modulation schemes, OFDM's results show really high benchmarks [8-10].

Although OFDM has many advantages and well performing qualities, due to its constructive nature when the signal is being formed, it has a serious problem regarding its Peak-to-Average-Power Ratio (PAPR). In particular, the high peaks of the signal may experience nonlinearity as the signal is pushed through a power amplifier, therefore distorting the signal and affecting the performance of the whole system [9, 11].

In this research, I will focus on the reduction of the PAPR of OFDM signal, show the result of the reduction, compare the effect and the efficiency of the methods used to conduct the reduction. In chapter II, an overview and some basic analysis of OFDM systems will be discussed. In chapter III, the methods used in the research will be described and implemented. In chapter IV, relevant results will be shown.

CHAPTER II

OFDM ANALYSIS

OFDM Overview

A simple OFDM system model is shown in Figure 1.

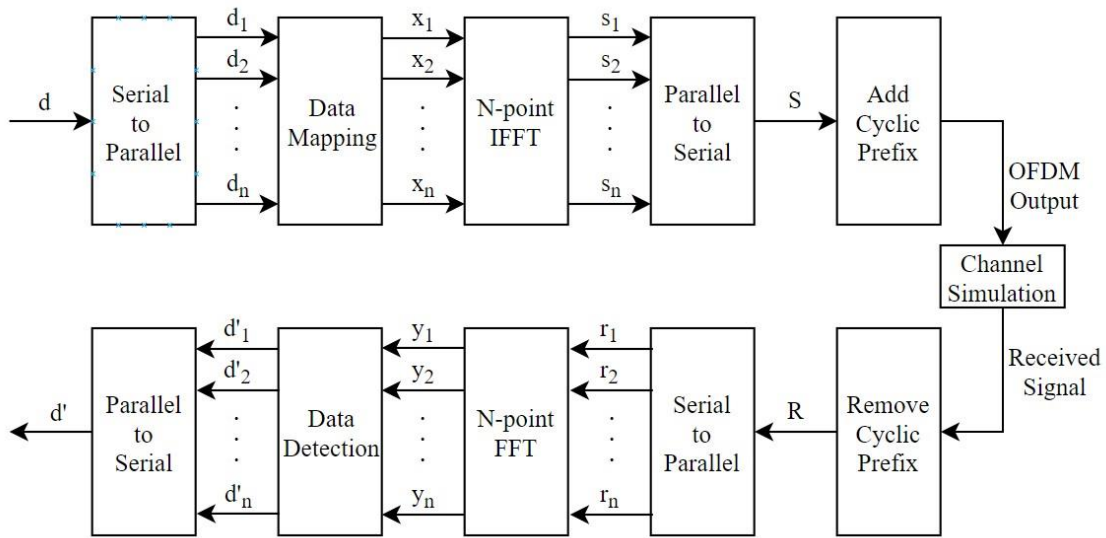


Figure 1 OFDM System Model

Let d represent a stream of binary data to be transmitted. First, the data stream is divided into n groups of size m bits by a serial to parallel converter, where n is the number of subcarriers, $m = \log_2 M$, and M represents size of the constellation map used to modulate the data. Some common modulation methods are Phase-Shift Keying (PSK) and Quadrature Amplitude modulation (QAM). The modulated data are represented by

the vector x of size n and each component $x(k)$ corresponds to the symbol transmitted over the k -th subcarrier.

Then an n -point Inverse Fast Fourier Transform (IFFT) is performed onto x . The output signal is calculated as the following equation:

$$S(j) = \frac{1}{n} \sum_{k=1}^n x(k) \left(e^{\frac{2\pi i}{n}} \right)^{(j-1)(k-1)} \quad (1)$$

The IFFT formula (1) can also be written as a matrix multiplication

$$S = \frac{1}{n} \cdot W_n \cdot x \quad (2)$$

where W_n is called the IFFT matrix

$$W_n = \left\{ \begin{array}{ccccc} w^0 & w^0 & w^0 & \dots & w^0 \\ w^0 & w^1 & w^2 & \dots & w^{n-1} \\ w^0 & w^2 & w^4 & \dots & w^{2(n-1)} \\ \vdots & \vdots & \vdots & \ddots & \vdots \\ w^0 & w^{(n-1)} & w^{2(n-1)} & \dots & w^{(n-1)(n-1)} \end{array} \right\}, w = e^{\frac{2\pi i}{n}} \quad (3)$$

Before the signal is transmitted, an extra layer of interference protection is added in the form of a Cyclic Prefix (CP). By repeating the end of the signal in an appropriate length, Inter-Symbol Interference (ISI) can be mitigated to a certain degree [12].

When the signal is received at the receiver, the CP is discarded and a n -point Fast Fourier Transform (FFT) is performed on the remaining segment of the signal.

$$Y(j) = \sum_{k=1}^n r(k) \left(e^{\frac{-2\pi i}{n}} \right)^{(j-1)(k-1)} \quad (4)$$

where the last part can be written as an FFT matrix similar to (3)

Each point in the array $Y(j)$ is then decoded to binary data by reverse mapping the point to its closest constellation point. In the presence of noise, the decoded constellation points could cross over to a wrong region and be interpreted wrongly, thus causing an error. This can be measured by symbol error rate, which is the ratio of symbol errors to the total number of symbols in relation to the amount of noise present. It is highly correlated to the SNR presented in the transmission channel.

Initial Analysis

The PAPR is not dependent on the constellation maps used in the OFDM system. In Table 1, PAPR statistics for some common constellation maps with 72 subcarriers are presented.

| (dB) | Average | Maximum | Minimum | Standard Deviation |
|--------|---------|---------|---------|--------------------|
| QPSK | 7.53 | 11.96 | 4.60 | 0.88 |
| 16QAM | 7.50 | 11.83 | 4.58 | 0.92 |
| 64QAM | 7.48 | 11.64 | 4.66 | 0.94 |
| 256QAM | 7.51 | 11.96 | 4.46 | 0.93 |

Table 1 PAPR Statistics for QPSK, 16QAM, 64QAM, 256QAM with 72 subcarriers

Given the same number of subcarriers, all constellation maps show similar average, maximum and minimum PAPR. As the number of subcarriers increase, the PAPR increases logarithmically [13].

CHAPTER III

METHODS

Previous Suppression Methods

There have been many methods proposed: block coding [14], clipping and filtering [15], insertion [16] and partial transmit sequence (PTS) [17], etc. Block coding can lower the PAPR by coding the data bits into codewords that are designed to have lower PAPR, but the added length on the codewords would result in lower data rate [14]. PTS among other phase control methods multiplies the signal by phase factors to produce a low PAPR, distortion can be avoided in this method, however extra side information is needed so the receiver can correctly decode the signal, and it will slow down the bit rate and potentially degrade the performance [17].

Most of these methods require a change to the existing standards to work properly, in particular the receiver needs to adjust for the additional information to decode the data correctly. Since this is unlikely to occur, methods that only alter the signal or the input without extra information are more probable. Clipping and filtering is a good example of such methods. After the signal is created through IFFT, the peaks are reduced by cutting off excessive power above an assigned threshold. However, this will create distortion across all frequency components. The undesired information outside the designated frequencies could be negated by filtering the signal. But the distortion within the specified frequencies will affect the constellation points adversely, causing them to

change their positions and reducing their margin of error. Therefore, an increase in the error rate is an uncontrollable side effect to this method.

Basic Suppression Technique

The disadvantage of moved constellation points inspired a different approach to the problem of PAPR reduction. Since moving the constellation points is unavoidable, this approach views the movement of these constellation points as the main component of reducing the peak power. The new signal is formed by taking the IFFT of the modified constellation points as before, and the receiver would be able to decode the signal into these modified constellation points by an FFT. Therefore, it requires no side information or change to the receiver, so it can be implemented into existing standards and protocols.

Three methods of such approach will be discussed: Single Peak Suppression Method, Gradient Descent Method, and Newton's Method. The problem can be viewed as a constrained optimization problem: reduce the peaks by moving the constellation points, subject to a constraint on the allowed deviation in the constellation points. Previously, this has been studied by customizing the problem so Interior-Point Method (IPM) can be used to reach the optimal solution [18]. Gradient Descent and Newton's Method are common numerical methods to find solutions to optimization problems. They are alternative methods to IPM at solving optimization problems. They both require some modifications to the problem as IPM did before they can be implemented. The details of such modifications will be discussed in a later section.

Besides the constellation points, the IFFT matrix is the other major part of the formula in (2). Its size and content are dependent on the desired resolution of the output signal. However, the peak power of the output signal from an n -point IFFT may not represent the true peak of its equivalent continuous-time signal, therefore it is necessary to oversample the output signal. Typically, it is enough to oversample the signal by 4-times to find a relatively accurate PAPR [19].

In order to keep the average power at 1, the scaling factor before the IFFT matrix is changed to $\frac{1}{\sqrt{n}}$ and it is now a part of the IFFT matrix, which will now be a l by n matrix to compensate for the oversampling, with l being the oversampled IFFT length.

$$W_{l*n} = \frac{1}{\sqrt{n}} * \begin{pmatrix} w^0 & w^0 & w^0 & \dots & w^0 \\ w^0 & w^1 & w^2 & \dots & w^{n-1} \\ w^0 & w^2 & w^4 & \dots & w^{2(n-1)} \\ \vdots & \vdots & \vdots & \ddots & \vdots \\ w^0 & w^{(l-1)} & w^{2(l-1)} & \dots & w^{(l-1)(n-1)} \end{pmatrix}, w = e^{\frac{2\pi i}{l}} \quad (5)$$

Thus, the updated formula to calculate the signal is

$$S = W_{l*n} \cdot x \quad (6)$$

Single Peak Suppression

Description

Single Peak Suppression (SPS) is the simplest method out of the three. The peak is identified and lowered to a desired threshold. Then another peak is identified and lowered to a desired threshold. Then the process repeats until there are no more peaks above the threshold.

Let the peak power P_p fall on the j -th element in the signal S , the peak power is calculated according to (7)

$$P_p = |S(j)|^2 = |W(j) * x|^2 \quad (7)$$

Where $W(j)$ is the j -th row of the extended IFFT matrix (5).

If the desired threshold is denoted by P_t , then the new modified constellation points x' must satisfy the following equation

$$|S'(j)|^2 = |W(j) * x'|^2 = P_t \quad (8)$$

Where $x' = x + \beta * v$ with β being the step size, and v being the step direction.

The calculation of step size and step direction will be discussed in the following section. The new constellation points can be found and will act as the new starting point for the next iteration. Then the procedure continues by identifying the next peak and finding the next step size and step direction.

Calculation and MATLAB Implementation

The step direction for this algorithm will be the vector that represents the steepest descent, which is the negative gradient of $|S(j)|^2$

$$v = -2 * S(j) * \overline{W(j)} \quad (9)$$

Next, by substituting v into x' , (8) transforms into the following

$$|S(j)(1 - 2\beta)|^2 = P_t \quad (10)$$

Then the step size can be solved as

$$\beta = \frac{1}{2} \left(1 - \frac{\sqrt{P_t}}{\sqrt{P_p}} \right)$$

With the gradient and step size calculated, the modified constellation points can be found and the peak can be suppressed. However, the average power will be inevitably brought down as one peak is suppressed. So, to combat this, the signal is normalized after the peak is suppressed. But doing so will bring up the suppressed peak over the desired level. Therefore, in order to keep the peak lower than the desired threshold after normalization, P_t needs to be slightly lower than the desired level. Let p represent the lowered amount. In chapter IV, different values of p are considered to show the affect it has on the method's output and efficiency.

The MATLAB function can now be realized and the results will be discussed in the following chapter.

Gradient Descent Method

Description

The general steps for Gradient Descent are as follows: with a predetermined starting point, the gradient is first calculated. Then the method searches along the direction of negative gradient of the cost function. Next, an appropriate step size is determined. Lastly the new point of interest is found by subtracting the product of the search direction and the step size from the original point. The algorithm repeats these three steps until a stopping criterion is met.

Problem Modification and Calculation

The problem can be expressed mathematically as the following:

$$\text{minimize} \quad \max(|S|^2) \quad (11)$$

$$\text{subject to} \quad |x - x_o|^2 \leq \epsilon \quad (12)$$

$$E[|S|^2] > 1 \quad (13)$$

where S is the left-hand side of the equation (6), x is the current vector of modified constellation points, x_o is the vector of original constellation points, and ϵ is the upper bound of total deviation and can be any real positive number.

(13) is the average power constraint. As mentioned before, the average power will shift when the constellation points are moved. To benefit the PAPR, the new average power needs to be larger than the original average power.

In order to be able to apply Gradient Descent, the cost function needs to be differentiable. Therefore, the cost function (11) needs to be modified so that it is differentiable and retains the same output. This can be achieved by the softmax, or the log-sum-exp function. There are methods discovered and tested to improve upon the basics of softmax [20], however they include extra calculations which are not necessary for this problem. The new cost function now looks like the following:

$$\text{minimize} \quad \frac{1}{\alpha} \log \left(\sum_{i=1}^l e^{\alpha |S(i)|^2} \right) \quad (14)$$

The softmax function utilizes the advantage that, in most cases, the output signal has one dominant maximum: every value in the signal is first either increased or decreased exponentially, leaving the maximum value dominating the sum, and the log

operation will return a value that is slightly higher than the maximum of the signal. The variable $\alpha(\gg 1)$ helps further amplify bigger values in the signal, whereas the smaller values will not be affected too much. By having an α large enough, the result of the new cost function (14) is effectively the same as the old cost function (11). It is also easy to see that this function is indeed differentiable.

Next, Log Barrier Method [18] is applied to both constraints because Gradient Descent does not take constraints into account. Before that can be done, both constraints need to be modified to accommodate the step size calculation.

Let x_o be the original constellation points, then let $z = x - x_o$ be the current modification vector (initially $z = 0$). Then, with the previous assumption of x' , β , and v . The next iteration of modification vector is $z' = x' - x_o = z + \beta * v$.

With the above definitions, the deviation constraint (12) now looks like

$$|z|^2 \leq \epsilon \quad (15)$$

It can be assumed that the best solution to minimize PAPR will be such that $|z|^2 \approx \epsilon$.

More importantly, all modification vector including the next iteration of the modification vector must satisfy (15) as well, hence

$$|z'|^2 = |z + \beta * v|^2 \leq \epsilon \quad (16)$$

By expanding and then using quadratic formula, the upper bound for step size derived from the deviation constraint will come out as

$$\beta \leq \frac{-2\text{Re}[z \cdot v] + \sqrt{(2\text{Re}[z \cdot v])^2 - 4|v|^2 * (|z|^2 - \epsilon)}}{2|v|^2} \quad (17)$$

There is a lower bound to the step size that will be negative so it will be ignored as any positive step size will satisfy the constraint.

The power constraint (13) can now be rewritten like the following.

$$|x|^2 \geq |x_o|^2 \quad (18)$$

Upon expanding, with the assumption of $|z|^2 \approx \epsilon$

$$\text{Re}[x_o \cdot z] \geq -\frac{\epsilon}{2} \quad (19)$$

Then, because any future iteration must also satisfy this inequality as well, the following must be true as well

$$\begin{aligned} \text{Re}[x_o \cdot (z + \beta * v)] &\geq -\frac{\epsilon}{2} \\ \Rightarrow \beta * \text{Re}[x_o \cdot v] &\geq -\frac{\epsilon}{2} - \text{Re}[x_o \cdot z] \end{aligned} \quad (20)$$

Note the right-hand side of (20) will never be positive given (19) is true.

Next, one of the following two scenarios can happen.

$$1. \text{ If } \text{Re}[x_o \cdot v] \geq 0, \text{ then } \beta \geq \frac{-\frac{\epsilon}{2} - \text{Re}[x_o \cdot z]}{\text{Re}[x_o \cdot v]} \quad (21)$$

$$2. \text{ If } \text{Re}[x_o \cdot v] \leq 0, \text{ then } \beta \leq \frac{-\frac{\epsilon}{2} - \text{Re}[x_o \cdot z]}{\text{Re}[x_o \cdot v]} \quad (22)$$

In the first case, the right-hand side will always be negative, any positive step size will satisfy so the upper bound for the step size is (17). In the second scenario, the smaller value between (17) and (22) will be chosen as the upper bound for the step size. With a lower bound of 0 and an appropriate upper bound, the step size value that leads to the lowest output to the cost function (24) will be used and its corresponding set of modified constellation points will be the starting points for the next iteration.

With the step size calculation properly outlined, the two constraints also transformed nicely (15)(19) and can now be modified by Log Barrier Method

$$\phi(x) = -\frac{1}{u}(\log(\epsilon - |z|^2) - \log(\frac{\epsilon}{2} + Re[x_o \cdot z])) \quad (23)$$

Adding the log barriers (23) onto the cost function, the optimization problem can be stated as the following:

$$\text{minimize } \frac{1}{\alpha} \log \left(\sum_{i=1}^l e^{\alpha |s(i)|^2} \right) - \frac{1}{u} (\log(\epsilon - |z|^2) - \log(\frac{\epsilon}{2} + Re[x_o \cdot z])) \quad (24)$$

Now that the cost function is fully modified, the gradient of (24) can be calculated and the method can proceed.

MATLAB Implementation

To simulate this method in MATLAB and to keep the total execution time to a minimum, the function will run until it does not reduce the cost function anymore or 15 iterations are run in which case the current constellation points are returned.

Now all the necessary details are outlined. The following parameters are used in the realization of Gradient Descent function:

1. Softmax function parameter α is set to be 10.
2. Log Barrier function parameter is initially set to 10, and increasing multiplicatively by 3 every time the updated reduction amount is lower than 0.5dB; This is because if the initial value is set too high or too low, the method will sometimes stop too early when there is clear more room for improvement. With these two parameters, good reduction is possible in almost all cases.
3. Deviation constraint is set to 1. This is selected to limit the SNR increase at 1% error rate less than approximately 0.5dB. (Error rates graphs shown in Chapter IV)
4. 10 potential step sizes between the lower and upper bounds are chosen to be calculated and compared.

With these numbers specified, the MATLAB function can be fully realized, and the results will be shown in the next chapter.

Newton's Method

Description

Newton's Method is a second order optimization algorithm that utilizes the same concept as Gradient Descent. Through a different search direction, each iteration for Newton's Method will be much more efficient at finding the next minimum point.

Newton's method follows the same 3 steps as Gradient Descent. But instead of using the negative gradient as the search direction, the Hessian is calculated and the search direction is the negative of the product of the inverse Hessian matrix and the gradient.

Theoretically, this search direction makes the method more efficient at finding the optimal solution than Gradient Descent.

Calculation and MATLAB Implementation

The set-up for Newton's Method is identical to that of Gradient Descent. The gradient and the hessian matrix of the cost function (24) will be used to calculate the search direction. The step size calculation is the same as explained in Gradient Descent. But due to its huge computational cost as shown in chapter IV, the stopping criterion is set to 5 total iterations. The necessary parameters for the MATLAB function are also the same as used for the Gradient Descent function.

The MATLAB implementation can be realized and the results will be discussed in the next chapter.

CHAPTER IV

RESULTS

Most of the following results are concluded from OFDM simulations with QPSK mapping of 72 subcarriers. Because PAPR is independent from the mapping, QPSK is sufficient to show the effect of the peak reduction by all three methods. The number of subcarriers (72, 180, 300, 1200) used in this research is taken from LTE standards [21].

SPS Overshot

First, as mentioned in chapter III, to properly suppress the peaks, SPS needs to set the P_t lower than the desired threshold by p . A few numbers for p are selected and tested. Their results in terms of iterations to reach the optimal solution and the final PAPR are shown in Table 2 and 3. One iteration is defined as when the new constellation points are found and the new signal is produced.

| p (dB) | Average | Maximum | Minimum | Standard Deviation |
|----------|---------|---------|---------|--------------------|
| 0.1 | 32.73 | 88 | 11 | 9.34 |
| 0.2 | 27.16 | 55 | 10 | 7.26 |
| 0.5 | 22.31 | 45 | 9 | 5.65 |
| 0.8 | 21.01 | 43 | 9 | 5.91 |
| 1.0 | 20.71 | 41 | 9 | 4.87 |

Table 2 Iteration statistics for different values of p . 10,000 randomly generated signals were reduced with each value of p , and all with the threshold of 4dB.

| p (dB) | Average | Maximum | Minimum | Standard Deviation |
|----------|---------|---------|---------|--------------------|
| 0.1 | 3.9907 | 4.0000 | 3.9410 | 0.0078 |
| 0.2 | 3.9825 | 4.0000 | 3.9129 | 0.0147 |
| 0.5 | 3.9596 | 3.9999 | 3.7878 | 0.0364 |
| 0.8 | 3.9450 | 3.9999 | 3.6821 | 0.0476 |
| 1.0 | 3.9359 | 4.0000 | 3.6435 | 0.0560 |

Table 3 Final PAPR statistics for different values of p . 10,000 randomly generated signals were reduced with each value of p , and all with the threshold of 4dB.

It is easy to see that the suppressed PAPR show very similar characteristics. With the increase of p , the average does not change significantly. But as p goes from 0.1dB to 0.5dB, the average number of iterations reduces by a lot, while as p gets bigger than 0.5dB, the decrease in iterations required slows down. Therefore, to avoid over-suppressing the signal when it is not needed, the desired threshold will be overshoot by 0.5dB for the remaining simulation results.

PAPR Reduction

To show that all three methods can reach the same level of PAPR, Gradient Descent and Newton's Methods are executed first, and their average final PAPR was used as the desired level for SPS function. Figure 2 illustrates part of a randomly generated signal and its PAPR before and after the reduction via all three methods.

For this one randomly generated signal, Gradient Descent and Newton's Method produced very close PAPRs, 5.21dB and 5.12dB respectively. Since SPS's threshold was

to match the other two methods, all three final PAPRs were all similar to each other. Also, their final signals all present similar shapes. This can be generalized as the comparison between the results of all three methods. If SPS has a threshold on the same level as the other two methods, all final signals and PAPRs show similar characteristics.

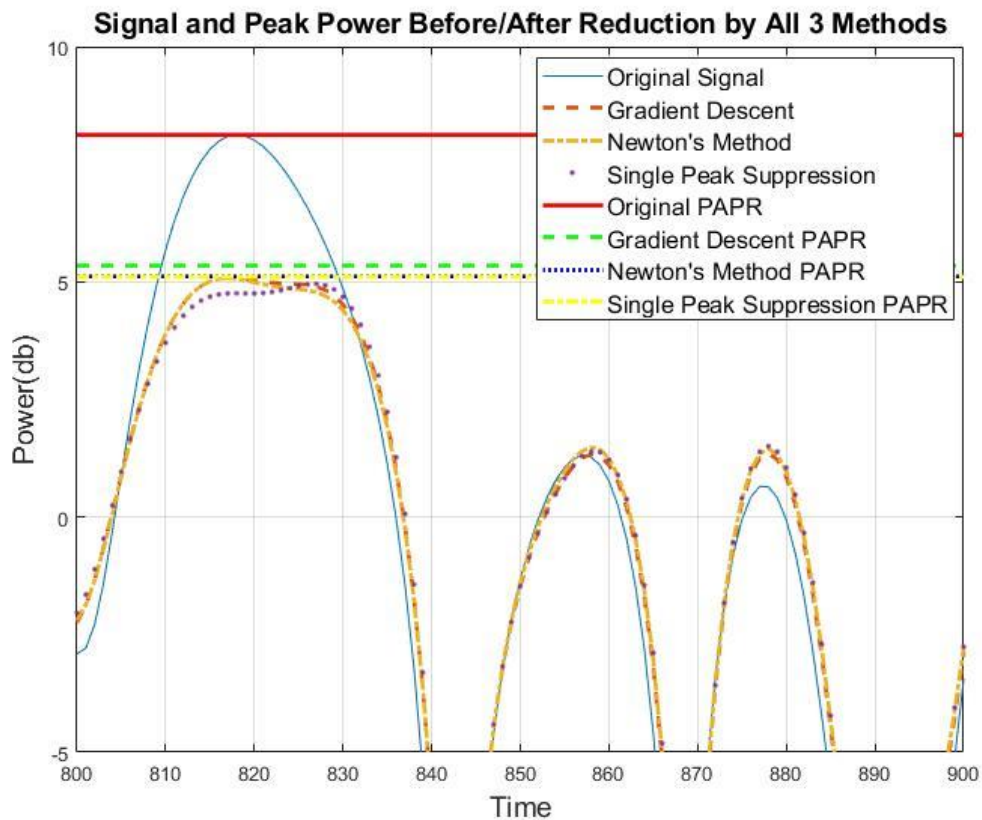


Figure 2 Part of a randomly generated signal before and after reduction. The threshold was the average final PAPR of Gradient Descent and Newton’s Method. All respective PAPRs are also shown. (72 subcarriers with QPSK)

To showcase the reduction consistency of all three methods, 10,000 data sequences were generated, and each sequence was reduced by all three methods. Table 4

shows PAPR statistics for all three methods. SPS produces the most consistent PAPR due to its goal of aiming for the same PAPR level (average of the averages for Gradient Descent and Newton’s Method) regardless of data. Gradient Descent and Newton’s Method show comparable results. Their similarities can be seen in their CCDF graphs shown in Figure 3.

| (dB) | Average | Maximum | Minimum | Standard Deviation |
|-------------------------|---------|---------|---------|--------------------|
| Gradient Descent | 5.23 | 10.15 | 3.27 | 0.69 |
| Newton’s Method | 5.10 | 9.81 | 3.30 | 0.65 |
| Single Peak Suppression | 5.13 | 5.16 | 4.66 | 0.07 |

Table 4 PAPR statistics post reduction by all three methods. 10,000 randomly generated signals were used. SPS used the average of the averages of Gradient Descent and Newton’s Method as the threshold and 0.5dB as the overshoot amount.

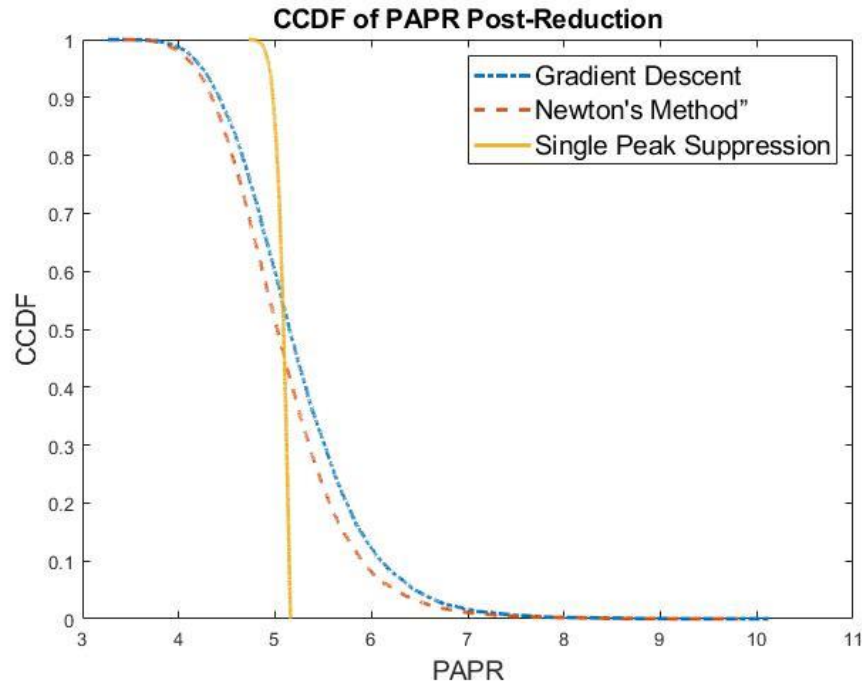


Figure 3 CCDF of the PAPR of the 10,000 signals shown in Table 4.

Reduction Efficiency

Gradient Descent and Newton’s Method follow the same principle. However, their difference in the search directions makes Newton’s Method more efficient at finding the optimal solution with each iteration. This can be shown in Figure 4, where the PAPR after each iteration for the two methods is recorded. Newton’s Method descent to a low PAPR in fewer iterations, whereas Gradient Descent’s reduction is smoother and steadier after the initial iteration.

SPS cannot be compared properly with Gradient Descent and Newton’s Method because it does not produce a desirable PAPR until all peaks are suppressed, therefore it is not included in this figure.

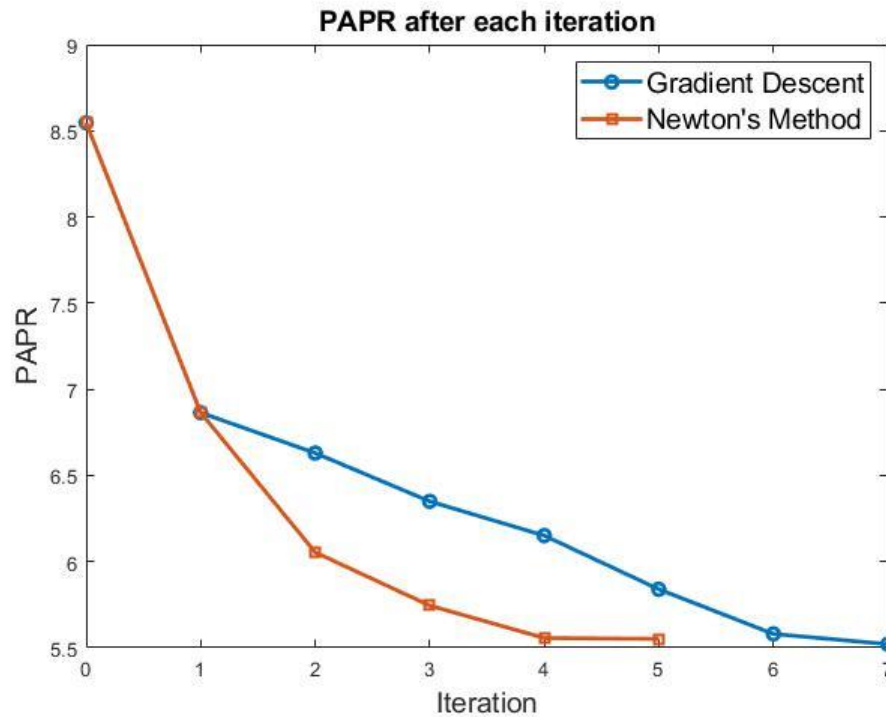


Figure 4 PAPR after each iteration of Gradient Descent and Newton’s Method.

Method Complexity

To fully understand the efficiency of each method, their complexities need to be evaluated. The complexity is measured in the number of operations per iteration. 3 operation types are tallied up and compared in Table 5. Complexity for typical clipping and filtering (assuming 12 iterations) [22] is included in the table to cast a comparison of the complexity between these proposed methods and an existing method.

| | Add./Sub. | Mul./Div. | Exp./Log./Other |
|-------------------------|-----------------|------------------|-----------------|
| Gradient Descent | $1440N^2+3480N$ | $2760N^2+3330N$ | 660N Exp. |
| Newton's Method | $380N^3+580N^2$ | $460N^3+1110N^2$ | 220N Exp. |
| Single Peak Suppression | $72N^2+108N$ | $144N^2+216N$ | 27 square roots |
| Clipping and Filtering | $192NF+96N$ | $192NF+96N$ | N.A. |

Table 5 Approximated number of operations for each category (real addition/subtraction; real multiplication/division; exponential/logarithmic and square roots) for all methods (including clipping and filtering). N = number of subcarriers, F = Finite Impulse Response (FIR) Filter Length

Assuming IFFT length is 4 times the number of subcarriers. The complexity for some calculation parts is summarized below

- 1) To calculate the gradient of (24), $24N^2 + 30N$ multiplications/divisions and $16N^2 + 20N$ additions/subtractions are needed.
- 2) The Hessian matrix and its inversion, assuming gaussian elimination method is used to invert the matrix, need about $92N^3 + 38N^2$ multiplication/divisions and $76N^3 + 20N^2$ additions/subtractions.
- 3) To find the best step size results requires $160N^2 + 192N$ multiplications/divisions and $80N^2 + 212N$ additions/subtractions.
- 4) Calculate the signal requires $16N^2 + 4N$ multiplications/divisions and $8N^2$ addition/subtractions.

Gradient Descent requires the calculation of 1) and 3), and the total complexity assumes 15 iterations. Newton's Method requires the calculation of 1), 2), and 3), and the total complexity assumes 5 iterations. The complexity for SPS is dominated by the renormalization of the signal as in 4), $20N$ multiplications/divisions and $12N$ additions/subtractions are needed to calculate its gradient and finding the new constellation points. The total complexity for SPS assumes 9 iterations.

The relative speed between the proposed three methods' iterations can be roughly proven by the average for total method execution time recorded in MATLAB shown in Table 6. However, this is not a true indicator as it depends on program and machine efficiency, but the MATLAB functions were written to be as efficient as possible so this is a relatively good representation of the three methods' speed.

| | Average Total Time(s) |
|-------------------------|-----------------------|
| Gradient Descent | 0.0256 |
| Newton's Method | 0.7821 |
| Single Peak Suppression | 0.0013 |

Table 6 Average time for each method's total time recorded in MATLAB.

Error Rate

The symbol error rate is computed by summing the likelihood of each symbol decoded as a wrong symbol when white additive white Gaussian noise (AWGN) is

present. In addition, Error Vector Magnitude (EVM) are calculated with each error rate graph. All three method's error rate graphs are show in the Figure 5.

The same data sequence that produced the result in Figure 2 was used. The error rate for all three methods are very similar. As noise level decreases, their difference becomes more noticeable, with Newton's Method being slightly better than Gradient Descent which is slightly better than SPS. The SNR increase at 1% error rate is about 0.5dB. This is consistent with the parameters used across all three methods.

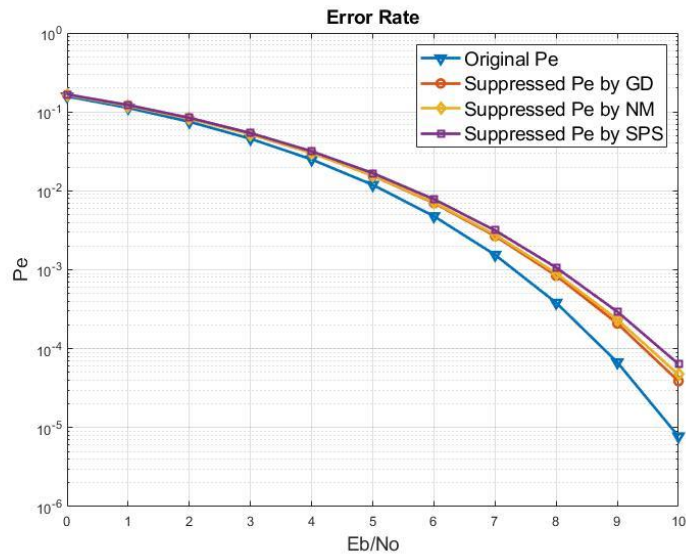


Figure 5 Error rate of the constellation points before and after reduction (72 subcarriers with QPSK). EVMs: -19.44dB (GD), -18.68dB (NM), -18.12dB (SPS).

Additional Results

All three methods are not specified to any constellation size. To illustrate that, 16QAM will be used instead of QPSK. Without changing any other parameters, the final PAPRs for all three methods are shown in Figure 6. And their respective error rates are shown in Figure 7.

To keep the error rates at 1%, signal power needs to be increased by 3dB, which makes the PAPR reduction (roughly 3dB) ineffective overall. This huge increase in error rate is due to the tight spacing between the constellation points, there are less room for the modified points to be affected by noise before they are decoded as wrong data symbols.

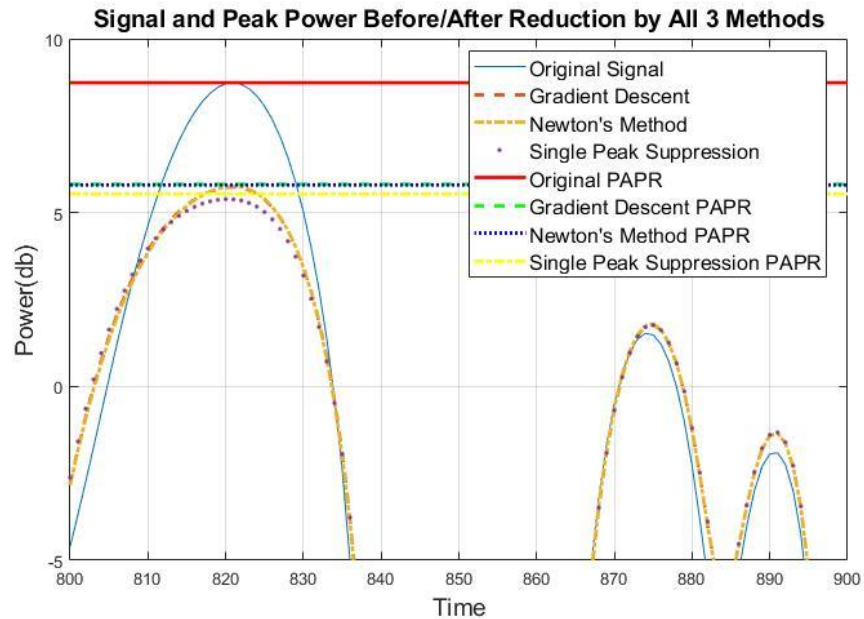


Figure 6 Part of a randomly generated signal before and after reduction (72 subcarriers with 16QAM). The respective PAPR is also shown.

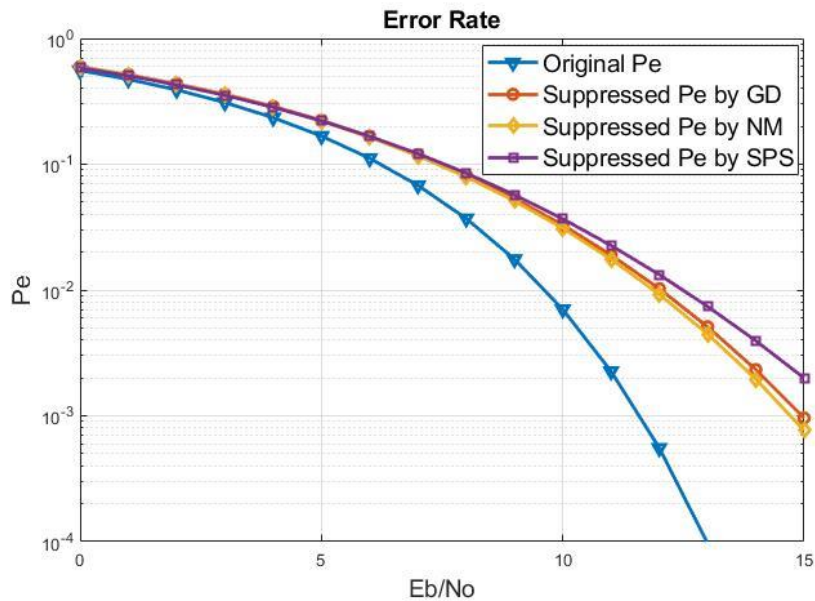


Figure 7 Error rate of the constellation points before and after reduction (72 subcarriers with 16QAM). EVMs: -18.57dB (GD), -18.69dB (NM), -17.50dB (SPS)

By increasing the number of subcarriers, each constellation point is allowed to move less which could potentially decrease the error rates. First, 180 subcarriers are considered. The reduced PAPRs and signals with 180 subcarriers are shown in Figure 8. The error rate shows improvement in Figure 9. But it can still be improved further (1dB signal increase at 1% error rate).

Next, 300 and 1200 subcarriers are used, and their respective error rates are shown in Figure 10. It can be assumed that all three methods would produce similar error rates as the number of subcarriers increase. Thus, only error rates from Gradient Descent is shown. Both curves exhibit acceptable SNR at 1% error rate.

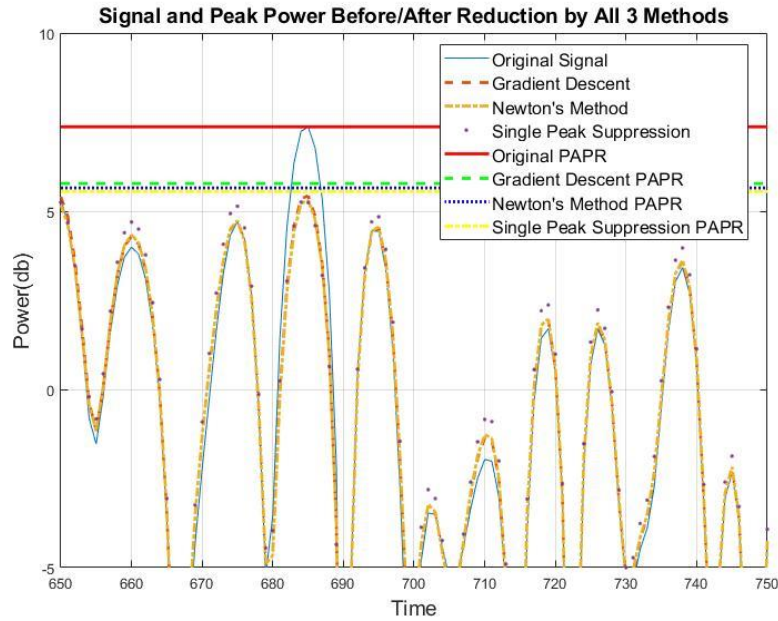


Figure 8 Part of a randomly generated signal before and after reduction (180 subcarriers with 16QAM). The respective PAPR is also shown.

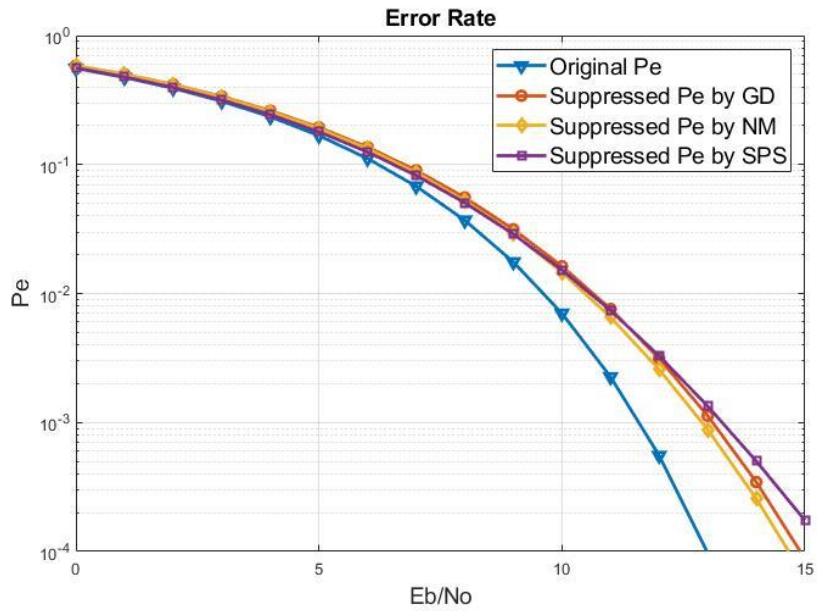


Figure 9 Error rate of the constellation points before and after reduction (180 subcarriers with 16QAM). EVMs: -22.56dB (GD), -23.20dB (NM), -21.11dB (SPS).

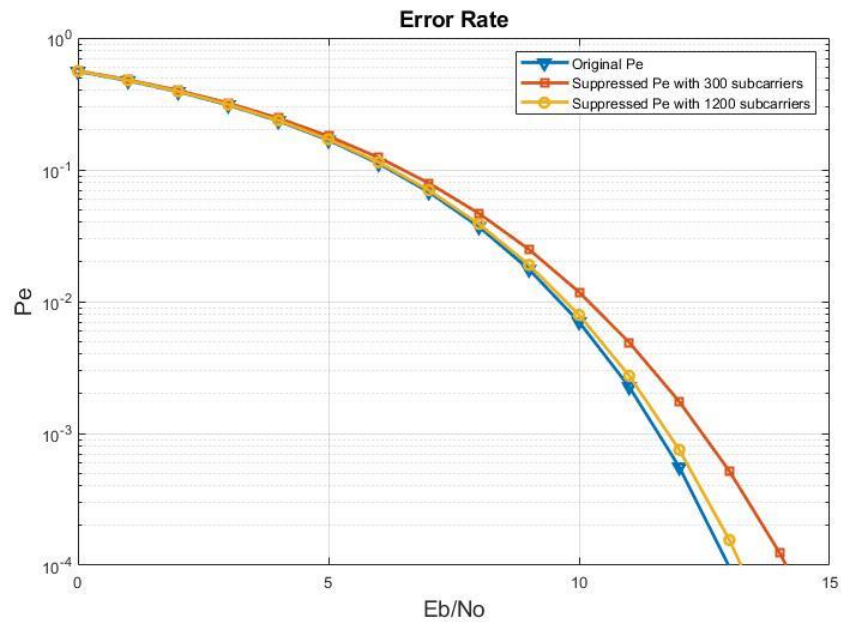


Figure 10 Error rate of the constellation points before and after Gradient Descent (300 and 1200 subcarriers with 16QAM). EVMs: -24.78dB (300), -30.80dB (1200).

Instead of changing the number of subcarriers, the total deviation ϵ can be lowered to achieve the same effect. The result with $\epsilon = 0.2$ is shown in Figure 11 and Figure 12.

The PAPR reduction is expectedly smaller. But the error rates' improvement can be easily seen. Following the same reasoning, higher order constellation maps (64QAM and 256QAM) can be used and reduced by these methods with the appropriate number of subcarriers and deviation limit.

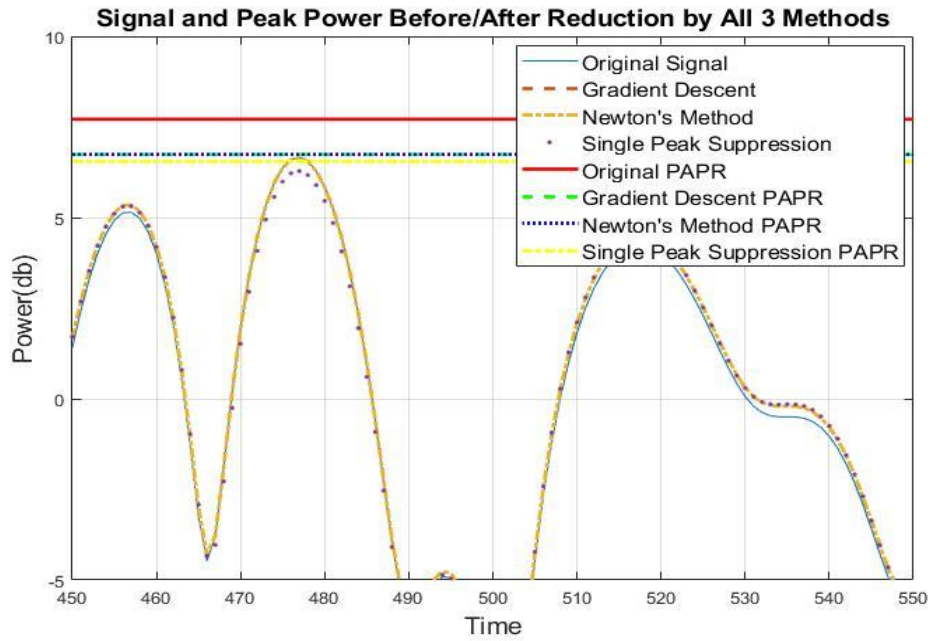


Figure 11 Part of a randomly generated signal before and after reduction (72 subcarriers with 16QAM, $\epsilon = 0.2$). The respective PAPR is also shown.

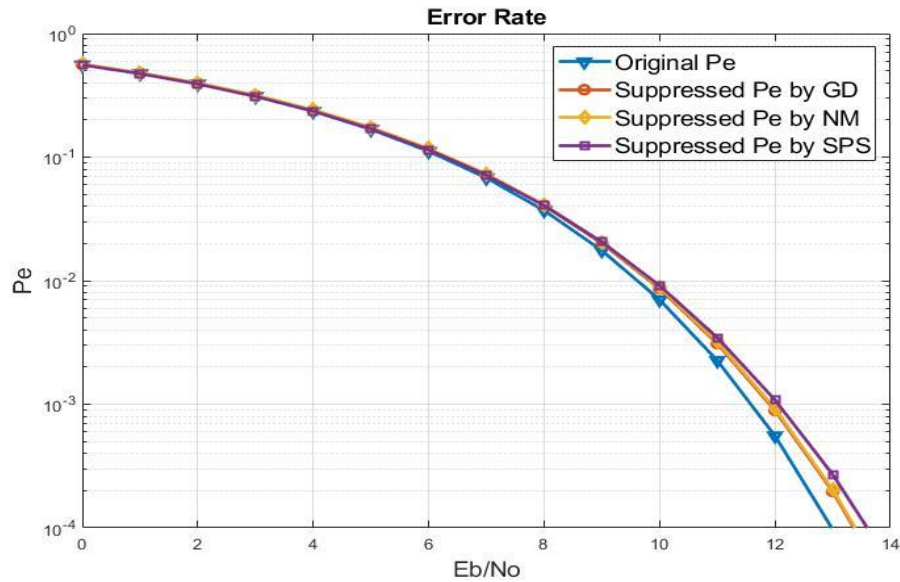


Figure 12 Error rate of the constellation points before and after reduction (72 subcarriers with 16QAM, and $\epsilon = 0.2$). EVMs: -28.58dB (GD), -28.67dB (NM), -26.13dB (SPS).

CHAPTER V

CONCLUSION

In this thesis, 3 PAPR reduction methods for the OFDM systems are provided. The most traditional methods cannot be realistically implemented in existing standard as most require extra side information. These methods focus on changing the mapped constellation points in order to manipulate the peak power. The 3 methods' algorithms are described in detail, including the modification to the problem in order to apply Gradient Descent and Newton's Method. Their simulation is done in MATLAB, and their reduction results are discussed.

To measure the method's effectiveness, a large number of samples are generated and their post reduction PAPR are compared. In addition, each method's complexity is summarized and roughly examined via the timing function in MATLAB. Each method's effect on error rate is also compared.

In conclusion, all three methods can be used to suppress any OFDM system. However, if the system has a large number of subcarriers, Newton's Method is not recommended due to its intense computational complexity. Gradient Descent has much less complexity and it can reach similar results as Newton's Method. But Single Peak Suppression can both suppress the signal most efficiently as it takes the least amount of operations in most scenarios.

REFERENCES

- [1] L. Cimini, "Analysis and Simulation of a Digital Mobile Channel Using Orthogonal Frequency Division Multiplexing," in *IEEE Transactions on Communications*, vol. 33, no. 7, pp. 665-675, July 1985.
- [2] F. B. Frederiksen and R. Prasad, "An overview of OFDM and related techniques towards development of future wireless multimedia communications," *Proceedings RAWCON 2002. 2002 IEEE Radio and Wireless Conference (Cat. No.02EX573)*, Boston, MA, USA, 2002, pp. 19-22.
- [3] M. Aldinger, "Multicarrier COFDM scheme in high bitrate radio local area networks," 5th IEEE International Symposium on Personal, Indoor and Mobile Radio Communications, Wireless Networks - Catching the Mobile Future., The Hague, Netherlands, 1994, pp. 969-973 vol.3.
- [4] P. Hoehner, J. Hagenauer, E. Offer, C. Rapp and H. Schulze, "Performance of an RCPC-coded OFDM-based digital audio broadcasting (DAB) system," *IEEE Global Telecommunications Conference GLOBECOM '91: Countdown to the New Millennium. Conference Record*, Phoenix, AZ, USA, 1991, pp. 40-46 vol.1.
- [5] de Bot, Paul G.M. "OFDM for Digital Terrestrial Television Broadcasting." DTTB: Orthogonal Frequency Division Multiplexing, www.wirelesscommunication.nl/reference/chaptr01/brdcsyst/dttb/dttb1.htm.
- [6] K. Riyazuddin, A. K. Sharma and P. Reddy, "Performance Evaluation of LTE OFDM System Using an Adaptive Modulation Scheme in Indoor and Outdoor

- Environment," *2017 International Conference on Recent Trends in Electrical, Electronics and Computing Technologies (ICRTEECT)*, Warangal, 2017, pp. 54-58
- [7] M. -. Ho, J. Wang, K. Shelby and H. Haisch, "IEEE 802.11g OFDM WLAN throughput performance," *2003 IEEE 58th Vehicular Technology Conference. VTC 2003-Fall (IEEE Cat. No.03CH37484)*, Orlando, FL, 2003, pp. 2252-2256 Vol.4.
- [8] M. Y. Ali, S. M. S. Alam, M. S. M. Sher, M. T. Hasan and M. M. Rahman, "Performance Analysis of OFDM in Wireless Communication," *2009 Fourth International Conference on Computer Sciences and Convergence Information Technology*, Seoul, 2009, pp. 903-906.
- [9] S. Merchan, A. G. Armada and J. L. Garcia, "OFDM performance in amplifier nonlinearity," in *IEEE Transactions on Broadcasting*, vol. 44, no. 1, pp. 106-114, March 1998.
- [10] Lobato, M. Kushnerov, A. Diaz, A. Napoli, B. Spinnler and B. Lankl, "Performance comparison of single carrier and OFDM in coherent optical long-haul communication systems," *2011 Asia Communications and Photonics Conference and Exhibition (ACP)*, Shanghai, 2011, pp. 1-6.
- [11] P. Banelli and S. Cacopardi, "Theoretical analysis and performance of OFDM signals in nonlinear AWGN channels," in *IEEE Transactions on Communications*, vol. 48, no. 3, pp. 430-441, March 2000.

- [12] W. Henkel, G. Taubock, P. Odling, P. O. Borjesson and N. Petersson, "The cyclic prefix of OFDM/DMT - an analysis," 2002 International Zurich Seminar on Broadband Communications Access - Transmission - Networking (Cat. No.02TH8599), Zurich, Switzerland, 2002, pp. 22-22.
- [13] N. Dinur and D. Wulich, "Peak-to-average power ratio in high-order OFDM," in *IEEE Transactions on Communications*, vol. 49, no. 6, pp. 1063-1072, June 2001.
- [14] A. E. Jones, T. A. Wilkinson and S. K. Barton, "Block coding scheme for reduction of peak to mean envelope power ratio of multicarrier transmission schemes," in *Electronics Letters*, vol. 30, no. 25, pp. 2098-2099, 8 Dec. 1994.
- [15] Xiaodong Li and L. J. Cimini, "Effects of clipping and filtering on the performance of OFDM," in *IEEE Communications Letters*, vol. 2, no. 5, pp. 131-133, May 1998.
- [16] Heung-Gyoon Ryu, Jae-Eun Lee and Jin-Soo Park, "Dummy sequence insertion (DSI) for PAPR reduction in the OFDM communication system," in *IEEE Transactions on Consumer Electronics*, vol. 50, no. 1, pp. 89-94, Feb. 2004.
- [17] A. D. S. Jayalath, C. Tellambura and H. Wu, "Reduced complexity PTS and new phase sequences for SLM to reduce PAP of an OFDM signal," VTC2000-Spring. 2000 IEEE 51st Vehicular Technology Conference Proceedings (Cat. No.00CH37026), Tokyo, Japan, 2000, pp. 1914-1917 vol.3.

- [18] A. Aggarwal and T. H. Meng, "Minimizing the Peak-to-Average Power Ratio of OFDM Signals Using Convex Optimization," in *IEEE Transactions on Signal Processing*, vol. 54, no. 8, pp. 3099-3110, Aug. 2006.
- [19] M. Sharif, M. Gharavi-Alkhansari and B. H. Khalaj, "New results on the peak power of OFDM signals based on oversampling," 2002 IEEE International Conference on Communications. Conference Proceedings. ICC 2002 (Cat. No.02CH37333), New York, NY, USA, 2002, pp. 866-871 vol.2.
- [20] S. Zhang, C. Tepedelenlioğlu, M. K. Banavar and A. Spanias, "Max-consensus using the soft maximum," 2013 Asilomar Conference on Signals, Systems and Computers, Pacific Grove, CA, 2013, pp. 433-437.
- [21] "Frame Structure - Downlink." ShareTechnote, sharetechnote.com/html/FrameStructure_DL.html.
- [22] Y. Rahmatallah and S. Mohan, "Peak-To-Average Power Ratio Reduction in OFDM Systems: A Survey And Taxonomy," in *IEEE Communications Surveys & Tutorials*, vol. 15, no. 4, pp. 1567-1592, Fourth Quarter 2013.